PHYSICAL REVIEW B **75**, 241407(R) (2007)

SU(2) and SU(4) Kondo effects in carbon nanotube quantum dots

A. Makarovski,[1] A. Zhukov,[1] J. Liu,[2] and G. Finkelstein[1]
[1]*Department of Physics, Duke University, Durham, North Carolina 27708, USA*
[2]*Department of Chemistry, Duke University, Durham, North Carolina 27708, USA*
(Received 26 March 2007; published 25 June 2007)

We study the SU(4) Kondo effect in carbon nanotube quantum dots, where doubly degenerate orbitals form four-electron "shells." The SU(4) Kondo behavior is investigated for one, two, and three electrons in the topmost shell. While the Kondo state of two electrons is quenched by a magnetic field, in the case of an odd number of electrons two types of SU(2) Kondo effect may survive. Namely, the spin SU(2) state is realized in a magnetic field parallel to the nanotube (inducing primarily orbital splitting). Application of the perpendicular field (inducing Zeeman splitting) results in the *orbital* SU(2) Kondo effect.

DOI: 10.1103/PhysRevB.75.241407 PACS number(s): 73.23.Hk, 75.20.Hr, 73.63.Fg

At low temperatures, a variety of nanoscale Coulomb blockade[1] systems with degenerate ground states exhibit the Kondo effect.[2] This many-body phenomenon has now been observed in semiconductor quantum dots, molecules, carbon nanotubes, and magnetic addatoms on metallic surfaces (see Ref. 3 for a review). In high-quality nanotubes the quantum-mechanical orbitals originating in two electronic subbands are doubly degenerate, forming four-electron "shells"[4,5] (see also Ref. 6 for additional references). In each shell, the Kondo behavior develops in the valleys with one, two, and three electrons.[4,7] The Kondo effect with one electron in a shell is expected[8] to obey the SU(4) symmetry,[9,10] as studied recently in Ref. 11. In this paper, we investigate the SU(4) Kondo effect in the one-, two-, and three-electron valleys in a magnetic field.

The nanotubes are grown on a Si/SiO_2 substrate by chemical vapor deposition using CO as a feedstock gas.[12] This method was verified to produce mostly single-wall nanotubes with diameters of about 2 nm. Cr/Au electrodes separated by 200 nm (Figs. 1–3) or 600 nm (Fig. 4) are deposited on top of the nanotubes. All the measurements are conducted at temperatures between 1.2 K and 2 K. We choose to work with several small-gap semiconducting nanotubes,[13] which demonstrate high *p*-type conductance at negative gate voltages. At positive gate voltages, the middle section of the nanotube fills with electrons. The part of the nanotube adjacent to the electrodes stays *p*-type ("leads"). Therefore, a quantum dot is formed *within* a nanotube, defined by *p*-*n* and *n*-*p* junctions. As a result, a Coulomb blockade sets in at low temperatures (Fig. 1).

Figure 1 shows conductance map of a 200-nm-long nanotube quantum dot measured as a function of the source-drain bias V_{SD} and gate voltage V_{gate}. The "Coulomb diamonds"[1] demonstrate clear four-electron shell filling. The *p*-*n* junction transparency grows with V_{gate}, resulting in an enhancement of the Kondo effect in each successive shell. The zero-bias Kondo ridge appears in Coulomb diamonds with one, two, and three electrons (visible for $V_{gate}>10$ V).

The ambipolar semiconductor nanotubes as studied here are uniquely suited for observation of the SU(4) Kondo effect: the electrons are reflected adiabatically from the *p*-*n* junctions at the ends of the quantum dot, resulting in little mode mixing. Therefore, the level mismatch between the two orbitals level in a shell is very small, as evidenced by observation of the Kondo ridge in the 2*e* valleys of many successive shells (Fig. 1). It is also important for the observation of the SU(4) symmetry that the "leads" to the dot are formed within *the same nanotube* and thus have the same orbital symmetry, which should be conserved in tunneling processes.[8]

In nanotubes, the parallel magnetic field $B_{\parallel}$ couples to both the spin and orbital magnetic moments of electrons.[13–15] The orbital magnetic moment μ corresponding to the electron motion around the nanotube circumference is significantly larger than the spin magnetic moment μ_0 (we estimate $\mu \approx 7\mu_0$; see below). Therefore, in a magnetic field the levels in a four-electron shell should spilt into two doublets moving up or down in energy with $B_{\parallel}$. Each doublet corresponds to an orbital with a clockwise or counterclockwise direction of rotation with respect to the magnetic field, occupied by two electrons [spin up and spin down, schematic in Fig. 2(a)]. Exactly this behavior is observed in Fig. 2(a), which shows the conductance of a 200-nm-long nanotube quantum dot as a function of the gate voltage and parallel magnetic field. Three four-electron shells are visible in zero field, which are split into pairs of doublets in $B_{\parallel}$.

Figure 2(b) demonstrates conduction maps measured as a function of V_{SD} and V_{gate} at $B_{\parallel}=3$ T. The Kondo ridges split at finite field in several horizontal lines at finite V_{SD} (indicated by triangles) visible inside the Coulomb diamonds. These lines mark inelastic cotunneling thresholds; their ap-

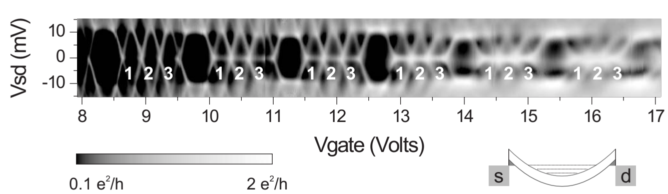

FIG. 1. Differential conductance map of a 200-nm-long semiconducting nanotube quantum dot measured as a function of V_{gate} and V_{SD} [grayscale map: $(0.1-2)e^2/h$; $T=2$ K, $B=0$]. "Coulomb diamonds" demonstrate four-electron periodicity. Six such four-electron shells are visible. Contact transparency grows with V_{gate}. For $V_{gate}>10$ V, the Kondo ridge is visible at $V_{SD}=0$ for one, two, and three electrons in the topmost shell. Schematic: the quantum dot is formed within the semiconducting nanotube.

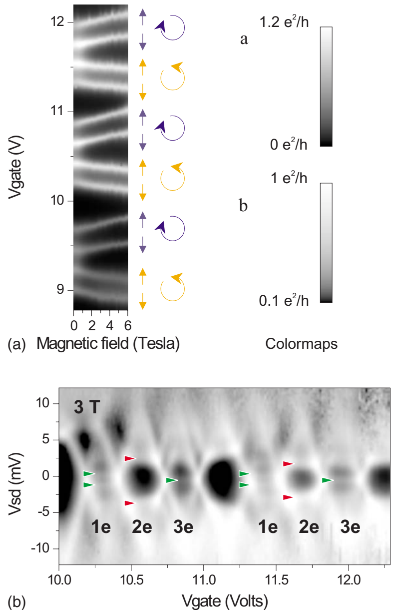

FIG. 2. (Color online) (a) Differential conductance of a 200-nm-long nanotube quantum dot (similar to Fig. 1) measured as a function of V_{gate} and $B_{\parallel}$. At zero field, three shells are visible. Within each shell, two lower (higher) single-electron traces move down (up) in a magnetic field. Each doublet corresponds to spin-up and spin-down electrons filling an orbital with a certain direction of rotation in magnetic field. Scale of the color map: $(0-1.2)e^2/h$. (b) Differential conductance map as a function V_{gate} and V_{SD} at $B_{\parallel}=3$ T. Two top shells of (a) are shown. In the $2e$ valleys, the zero-bias Kondo ridge splits into horizontal cotunneling features at $V_{SD}\approx\pm3$ meV (indicated by red/gray triangles), corresponding to an electron excitation from the lower to the higher orbital. The $1e$ valleys demonstrate two Zeeman-split features at $|V_{SD}|\lesssim 1$ meV, while the $3e$ valleys show a single feature close to zero bias (all indicated by green/light gray triangles). Grayscale: $(0.1-1.0)e^2/h$.

pearance indicates that the ground-state degeneracy is (partially) lifted. In the cotunneling processes, electrons tunnel in and out of the nanotube through a virtual state, leaving behind an excitation.[16] The energy of the excitation may be extracted from the value of $e|V_{SD}|$ at which a cotunneling feature is observed. The enhancement of the cotunneling thresholds, known as the out-of-equilibrium Kondo effect,[17–21] results in the appearance of peaks in the differential conductance [indicated by triangles in Fig. 2(b)].

The dependence of the cotunneling features on magnetic field can be best traced in Fig. 3, where we show the conductance measured as a function of V_{SD} and $B_{\parallel}$ in the three valleys. (In each field, the gate voltage is adjusted to stay in the centers of the $1e$, $2e$, or $3e$ valleys.) Let us consider the $2e$ valley first. There are six different low-energy states of the two electrons in the nanotube: three different singlet states and one three-component triplet state [schematic in Fig. 3(b)]. The energy differences between these states, due to the orbital mismatch, the exchange interaction, and the excess Coulomb interaction, are found to be very small.[6] In the presence of the lifetime broadening Γ, the states shown in Fig. 3(b) become effectively degenerate and all participate in the formation of the Kondo resonance. The Kondo state observed here in the two-electron valley is expected[22,23] to obey the SU(4) symmetry. It should be different from the two-electron singlet-triplet Kondo effect induced by level crossing in magnetic field,[24] where only four (and not six) degenerate states participate in the Kondo processes.[25]

As $B_{\parallel}$ is applied, the singlet state with two electrons occupying the lower orbital splits down from the rest [the lowest state in the schematic of Fig. 3(b)]. When the energy splitting becomes greater than the Kondo temperature ($\mu B_{\parallel} \sim k_B T_K$) at $B_{\parallel}\sim 1$ T, the zero-bias Kondo ridge disappears [Fig. 3(b)]. It is replaced by the inelastic cotunneling thresholds, which correspond to the excitation of the ground state and appear at $eV_{SD}=\pm 2\mu B_{\parallel}$ (one of the two electrons is moved from the lower to the higher energy orbital in the shell; see red arrows in the schematic of Fig. 3(b)]. These thresholds indeed evolve linearly with field and can be used to estimate the electron angular momentum as $\mu\approx 7\hbar$ and the diameter of the nanotube as 2 nm.[11,14]

In addition to the excitations at $\pm 2\mu B_{\parallel}$, the $1e$ and $3e$ valleys also demonstrate lower-energy features: two resonant cotunneling thresholds at $eV_{SD}\approx\pm g\mu_0 B_{\parallel}$ in the $1e$ valley [Fig. 3(a)] and a zero-bias peak in the $3e$ valley [Fig. 3(c)]. In both valleys, after the orbitals in the shell are split by more than the SU(4) Kondo temperature $T_K^{SU(4)}$, there is one electron left unpaired on the lower or the higher orbital, respectively. This electron can form the SU(2) Kondo state as long as $g\mu_0 B_{\parallel}\lesssim k_B T_K^{SU(2)}$. Apparently this scenario is realized in the $3e$ valley, resulting in the appearance of a single Kondo ridge close to zero bias [Figs. 2(b) and 3(c)]. If the SU(2) Kondo temperature is less than $g\mu_0 B_{\parallel}/k_B$, the SU(2) Kondo state is not formed and cotunneling features at $eV_{SD}\approx\pm g\mu_0 B_{\parallel}$ should appear, as seen in the $1e$ valley. A similar $1e$ behavior was recently observed and attributed[8,11] to the SU(4) Kondo effect.

We observe the difference between the $1e$ and $3e$ behaviors in several samples and for several cooldowns. At least in two samples, we can exclude the possibility of the two orbitals in a shell having different Γ, and hence different $T_K^{SU(2)}$. The effect was also found in successive shells [Fig. 2(b)], so a monotonic change of some parameter with V_{gate} may be ruled out. Overall, while we cannot explain the effect, it appears to be generic. Another open question presented by Fig. 3(a) concerns the low-energy cotunneling features. While at high fields their positions eV_{SD} are close to $\pm g\mu_0 B_{\parallel}$, at low fields they appear at energies significantly exceeding $\pm g\mu_0 B_{\parallel}$. In particular, the peaks seem to first emerge from the background at the energy of $eV_{SD}\sim k_B T_K^{SU(4)}$ (at $B_{\parallel}\approx 1.5$ T). The orbital cotunneling features are already well formed in this field. We believe these observations call for theoretical interpretations.

We find that the odd-electron valleys also exhibit cotunneling features whose energies *decrease* with field. These features are best visible in Fig. 3(c), in which case the electron occupying the higher orbital of the partially filled shell can be excited to the lower orbital of the next, unoccupied shell. The energy of such an excitation is $\Delta-2\mu B_{\parallel}$, where Δ is the splitting between the shells at zero field. This energy becomes lower in magnetic field, as the corresponding levels come closer. Extrapolating this energy to zero field, we find

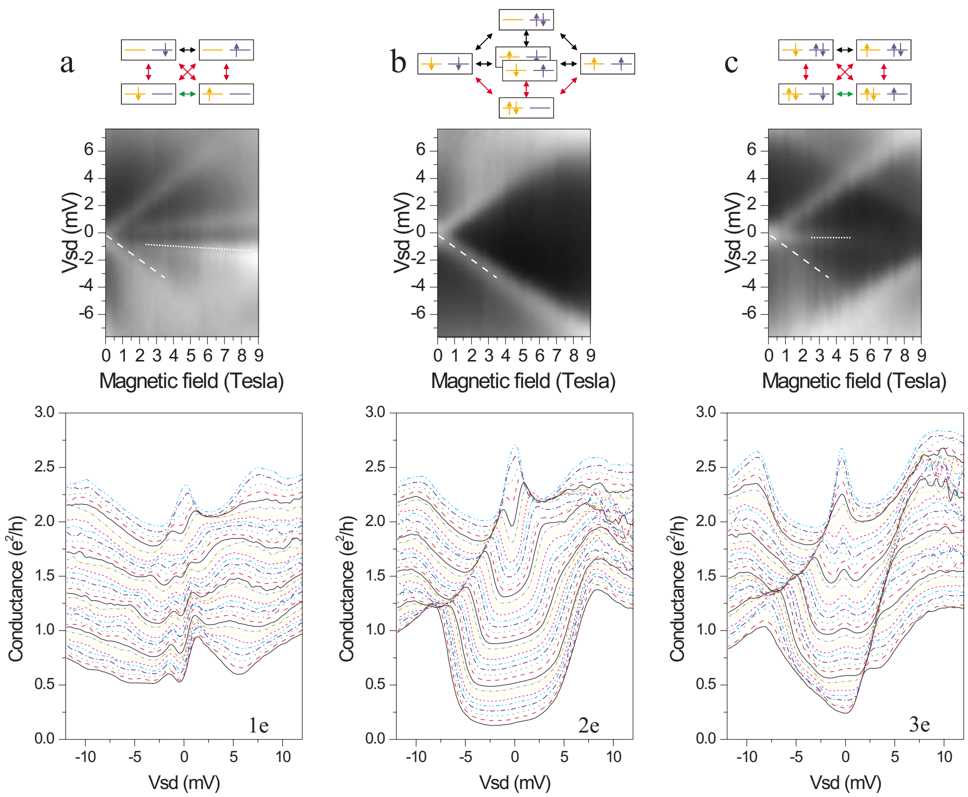

FIG. 3. (Color online) Dependence of the (a) $1e$, (b) $2e$, and (c) $3e$ Kondo features in perpendicular magnetic field. Top: schematics of the different states (rectangular boxes) and the allowed transitions induced between them by the tunneling processes (arrows). These states are degenerate at zero $B_{\parallel}$, but are split in the field. The lower row represents the states with the lowest orbital energies. The transitions to the states with higher orbital energies are indicated by red/gray arrows. The transitions within the lowest-energy Zeeman doublets (for $1e$ and $3e$) are shown by green/light gray arrows. Grayscale maps: conductance as a function of V_{SD} and $B_{\parallel}$. The gate voltage was adjusted to stay in the center of a valley when the magnetic field was stepped. The Kondo zero-bias peak (visible at $V_{SD}=0$, $B_{\parallel}=0$) splits into four, two, and three features in the $1e$, $2e$, and $3e$ valleys, respectively. The larger energy cotunneling peaks in all three images, marked by dashed lines at negative V_{SD} (and the symmetric features at positive V_{SD}), correspond to the orbital splitting. In the $1e$ valley, the lower-energy features marked by a dotted line at negative V_{SD} (and the symmetric feature at positive V_{SD}) roughly correspond to the Zeeman splitting. In the $3e$ valley, the single peak close to zero bias marked by a dotted line survives to higher fields. Lower row: the same differential conductance data shown as a function of the V_{SD} at different $B_{\parallel}$ ranging from 0 T to 9 T in 0.25-T increments (top to bottom). The curves are offset by $0.05e^2/h$ per 0.25 T starting from 9 T.

$\Delta \approx 10$ meV, consistent with other measurements. Similarly, in the $1e$ valley, an electron can be excited from a lower, completely filled shell, to the lower orbital of the partially filled shell, which is occupied by one electron. This process also requires energy of $\Delta - 2\mu B_{\parallel}$ [the corresponding faint feature may be visible in Fig. 3(a)]. In contrast, in a two-electron valley the intershell processes have energy of at least Δ, so that no extra low-energy cotunneling features are observed.

Finally, in Fig. 4 we study the dependence of the Kondo conductance on magnetic field perpendicular to the nanotube axis, $B_{\perp}$. In this orientation, the field primarily couples to the electron spins.[15] As a result, in the $2e$ valley, the ground state becomes an electron triplet, with the two electrons occupying different orbitals. The Kondo peak is suppressed [Fig. 4(b), $B_{\perp} \sim 3$ T] and nonequilibrium Kondo (cotunneling) features appear at energies slightly above $\pm g\mu_0 B_{\perp}$, corresponding to the spin-flip excitation of one of the electrons. In the $1e$ valley, on the other hand, the ground state remains degenerate in magnetic field: the electron can occupy one of two orbitals and we may expect to observe the orbital SU(2)

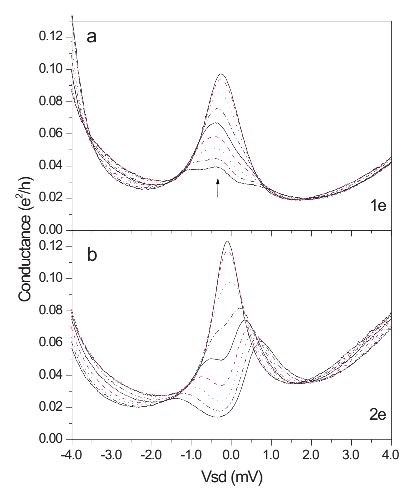

FIG. 4. (Color online) Conductance of a 600-nm-long nanotube quantum dot as a function of $B_{\perp}$ in the (a) $1e$ and (b) $2e$ valleys measured at different magnetic fields. $B_{\perp}$ ranges from 0 T to 8 T (top to bottom) in 1-T increments (the curves are not offset). The vertical arrow indicates the position of the orbital SU(2) peak in the one electron valley.

Kondo effect.[26] Indeed, the Kondo peak in Fig. 4(a) splits three ways: the two side peaks correspond to the spin-flip processes, while the center peak corresponds to the orbital SU(2) Kondo effect. The orbital (pseudospin) Kondo effect was observed earlier in double quantum dots.[27]

In conclusion, we study the transitions between the SU(4) and SU(2) Kondo temperatures in nanotube quantum dots in a magnetic field. The two-electron Kondo effect is suppressed by both parallel and perpendicular magnetic fields, due to formation of a nondegenerate ground state. In a parallel magnetic field, the odd-electron SU(4) Kondo may be completely suppressed or turn into the SU(2) (spin) Kondo effect. In a perpendicular magnetic field, the one-electron SU(4) Kondo effect is transformed to the SU(2) orbital Kondo effect.

We thank H. Baranger, A. Chang, L. Glazman, K. Le Hur, E. Novais, K. Matveev, G. Martins, M. Pustilnik, and D. Ullmo for valuable discussions. The work is supported by NSF Grant No. DMR-0239748.

[1] L. P. Kouwenhoven, C. M. Marcus, P. L. McEuen, S. Tarucha, R. M. Westervelt, and N. S. Wingreen, in *Mesoscopic Electron Transport*, edited by L. P. Kouwenhoven, G. Schon, and L. L. Sohn (Kluwer, Dordrecht, 1997), p. 105.

[2] A. C. Hewson, *The Kondo Problem to Heavy Fermions* (Cambridge University Press, Cambridge, England, 1993).

[3] L. P. Kouwenhoven and L. I. Glazman, Phys. World **14**, 33 (2001).

[4] W. J. Liang, M. Bockrath, and H. Park, Phys. Rev. Lett. **88**, 126801 (2002).

[5] M. R. Buitelaar, A. Bachtold, T. Nussbaumer, M. Iqbal, and C. Schonenberger, Phys. Rev. Lett. **88**, 156801 (2002).

[6] A. Makarovski, L. An, J. Liu, and G. Finkelstein, Phys. Rev. B **74**, 155431 (2006).

[7] B. Babic, T. Kontos, and C. Schonenberger, Phys. Rev. B **70**, 235419 (2004); **70**, 195408 (2004).

[8] M. S. Choi, R. Lopez, and R. Aguado, Phys. Rev. Lett. **95**, 067204 (2005).

[9] L. Borda, G. Zarand, W. Hofstetter, B. I. Halperin, and J. von Delft, Phys. Rev. Lett. **90**, 026602 (2003); G. Zarand, A. Brataas, and D. Goldhaber-Gordon, Solid State Commun. **126**, 463 (2003).

[10] K. Le Hur and P. Simon, Phys. Rev. B **67**, 201308(R) (2003); K. Le Hur, P. Simon, and L. Borda, *ibid.* **69**, 045326 (2004); R. Lopez, D. Sanchez, M. Lee, M. S. Choi, P. Simon, and K. Le Hur, *ibid.* **71**, 115312 (2005).

[11] P. Jarillo-Herrero, J. Kong, H. S. J. van der Zant, C. Dekker, L. P. Kouwenhoven, and S. De Franceschi, Nature (London) **434**, 484 (2005); Phys. Rev. Lett. **94**, 156802 (2005).

[12] B. Zheng, C. G. Lu, G. Gu, A. Makarovski, G. Finkelstein, and J. Liu, Nano Lett. **2**, 895 (2002).

[13] J. Cao, Q. Wang, M. Rolandi, and H. Dai, Phys. Rev. Lett. **93**, 216803 (2004).

[14] E. D. Minot, Y. Yaish, V. Sazonova, and P. L. McEuen, Nature (London) **428**, 536 (2004).

[15] T. Ando, Semicond. Sci. Technol. **15**, R13 (2000).

[16] D. V. Averin, and Yu. V. Nazarov, in *Single Charge Tunneling: Coulomb Blockade Phenomena in Nanostructures*, edited by H. Grabert, and M. H. Devore (Plenum Press, New York, 1992), p. 217.

[17] Y. Meir, N. S. Wingreen, and P. A. Lee, Phys. Rev. Lett. **70**, 2601 (1993).

[18] D. Goldhaber-Gordon, H. Shtrikman, D. Mahalu, D. Abusch-Magder, U. Meirav, and M. A. Kastner, Nature (London) **391**, 156 (1998); S. M. Cronenwett, T. H. Oosterkamp, and L. P. Kouwenhoven, Science **281**, 540 (1998); J. Schmid, J. Weis, K. Eberl, and K. Von Klitzing, Physica B **258**, 182 (1998).

[19] A. Kogan, S. Amasha, D. Goldhaber-Gordon, G. Granger, M. A. Kastner, and H. Shtrikman, Phys. Rev. Lett. **93**, 166602 (2004).

[20] D. M. Zumbuhl, C. M. Marcus, M. P. Hanson, and A. C. Gossard, Phys. Rev. Lett. **93**, 256801 (2004).

[21] J. Paaske, A. Rosch, P. Wolfle, C. M. Marcus, and J. Nygard, Nat. Phys. **2**, 460 (2006).

[22] M. R. Galpin, D. E. Logan, and H. R. Krishnamurthy, Phys. Rev. Lett. **94**, 186406 (2005).

[23] C. A. Busser and G. B. Martins, Phys. Rev. B **75**, 045406 (2007).

[24] S. Sasaki, S. De Franceschi, J. M. Elzerman, W. G. van der Wiel, M. Eto, S. Tarucha, and L. P. Kouwenhoven, Nature (London) **405**, 764 (2000).

[25] M. Pustilnik, L. I. Glazman, D. H. Cobden, and L. P. Kouwenhoven, Lect. Notes Phys. **579**, 3 (2001).

[26] A. L. Chudnovskiy, Europhys. Lett. **71**, 672 (2005).

[27] A. W. Holleitner, A. Chudnovskiy, D. Pfannkuche, K. Eberl, and R. H. Blick, Phys. Rev. B **70**, 075204 (2004).